

## ADAPTIVE SLIDING MODE GUIDANCE LAW WITH PRESCRIBED PERFORMANCE FOR INTERCEPTING MANEUVERING TARGET

MENGCHEN MA, KAI ZHAO AND SHENMIN SONG\*

Center for Control Theory and Guidance Technology  
Harbin Institute of Technology  
No. 92, West Da-Zhi Street, Harbin 150001, P. R. China  
mamengchenhit@163.com; 1014553342@qq.com  
\*Corresponding author: songshenmin@hit.edu.cn

Received April 2019; revised August 2019

**ABSTRACT.** *This paper describes sliding mode guidance laws with prescribed performance for maneuvering targets. The proposed guidance laws, which combine a novel error variable function with a new sliding mode surface, ensure that the line of sight (LOS) angle converges to the desired value and the LOS tracking error converges to an arbitrarily small residual set faster than some pre-designed rate. By combining the system tracking error with the prescribed performance function, a novel error variable function is designed and a new sliding mode surface is proposed. The key concept in this approach is to transform the prescribed performance constraint problem into that of the boundedness of the error variable function. The boundedness of the novel sliding mode surface ensures that the system state converges according to the prescribed performance. Additionally, this paper discusses the problem whereby the upper bound of the aggregate uncertainty, including the target information, is unavailable. An adaptive guidance law is presented for this scenario. Finally, simulation results are compared with those using other guidance laws. Numerical simulations show that the guidance laws presented in this paper achieve effective performance and can ensure the LOS angle converges to the desired value.*

**Keywords:** Prescribed performance, Error variable function, Sliding mode guidance law, Adaptive control

1. **Introduction.** In the problem of missile interception, the main objective of guidance laws is to allow missiles to intercept targets by ensuring a minimum miss distance [1]. In modern warfare, the combat capability of missiles can be enhanced by considering a specific impact angle [2,3]. There has been considerable research in this area. In 1973, Kim and Grider [4] designed a suboptimal terminal guidance system for reentry vehicles under an impact angle constraint. This guidance system was designed as a linear quadratic control problem. Kim et al. [5] developed a proportional navigation guidance law with a supplementary time-varying bias to satisfy the impact angle constraint. This bias compensated for target acceleration and sensor noise. An angle-constrained biased proportional navigation guidance (ACBPNG) law has been developed [6]. Considering that line of sight (LOS) rate control determines the angle of incidence, a closed loop was derived for ACBPNG and the exact bias for the required impact angle was determined. A biased pure proportional navigation guidance law has been proposed [7], and optimal guidance laws with angle constraints have been derived by transforming the impact angle constraint into an optimal control constraint problem [8-11]. Based on optimal control theory other forms of optimal guidance laws with angle constraints can be stated. For

instance, the direction of the missile can be adjusted to the optimal attack line, thus controlling the miss distance and the terminal angle, using the missile end position and speed deviation as state variables [12]. In recent decades, sliding mode control (SMC) theory has attracted widespread attention. For example, a terminal sliding mode guidance law in which the system state converges in finite time has been reported [13]. A nonsingular sliding mode guidance law [14] has been designed to solve the problem of singularities on the sliding mode surface. This ensures that, for any initial heading angle, the missile intercepts the target at a desired impact angle without exhibiting any singularity. Based on adaptive theory and a nonsingular fast terminal SMC method, an adaptive nonsingular fast terminal sliding mode guidance law was developed to allow the missile to intercept maneuvering targets [15]. In the problem of a missile intercept a stealth aircraft, the guidance law designed for this system should constrain the line of sight (LOS) angle during the whole guidance process as the radar cross section for stealth target can only be identified at a certain specific angle. In the coordinated operation of multiple missiles, due to the constraints of communication or cooperative detection, the spatial configuration between multiple missiles is required to meet certain constraints. Therefore, the state of the guidance system should converge according to certain prescribed performance criteria. In addition, the theory can be applied to such fields as spacecraft attitude control or robot control [16].

The literature review in the preceding paragraph demonstrates that, although there has been considerable research on guidance laws with angle constraints, most methods restrict the terminal LOS angle, which does not constrain the convergence process. To further analyze and research the control process, the state of the control system should converge according to some prescribed performance criteria. In this direction, the funnel control approach was proposed [17-19]. This is a continuation of the adaptive high-gain control methodology that replaces the monotonically increasing control gain with a time-varying function. When the output error of the system is close to the funnel boundary, the funnel control admits high values, resulting in a simple nonlinear and time-varying proportional control scheme for classes of nonlinear systems with a known relative degree of one [20-23] and, more recently, two [24,25]. In recent years, Bechlioulis and Rovithakis proposed prescribed performance control (PPC) theory. Based on a designed performance constraint function, a PPC controller was designed [26] by transforming the system tracking error into an equivalent unconstrained system through an error transformation. Furthermore, PPC has been used to design adaptive controllers for various classes of nonlinear systems. For instance, two robust adaptive controllers for single-input/single-output strict feedback nonlinear systems possessing unknown nonlinearities have been proposed [27]. These can ensure that the tracking error converges to an arbitrarily small residual set at a rate that is not less than a specified value, and that the maximum overshoot is not less than a small constant. A control scheme has also been designed for multi-input/multi-output affine control nonlinear systems with guaranteed prescribed performance [28]. Adaptive dynamic surface control technology was employed to design a PPC controller that satisfies the performance constraints of tracking error for a feedback system with a certain form [29].

In recent years, SMC has been widely used in controller design because of its strong robustness to external disturbances and the uncertainty of the system parameters [30]. With the development of hypersonic vehicles and other high speed missiles, the maneuver power of attacking targets is constantly increasing [31]. In the terminal guidance phase, the maneuver of the target is a major factor affecting the guidance accuracy [32]. To solve the problem of state constraints and make full use of the advantages of SMC, this paper presents sliding mode guidance laws with prescribed performance. Similar to the collision

avoidance function designed in [33], an error variable function is derived by combining the system state tracking error with a designed prescribed performance constraint function. The guidance law introduced in this paper is simpler and more robust than the methods discussed above.

The remainder of this paper is organized as follows. In Section 2, the guidance model considering target maneuvering is established. The prescribed performance constraint function and the error variable function are then designed. In Section 3, the sliding mode guidance law with prescribed performance is introduced. For the unknown upper bound of an external disturbance, an adaptive sliding mode guidance law is derived based on adaptive control theory. Simulation results and analyses are presented in Section 4. Finally, Section 5 summarizes our conclusions.

## 2. Problem Formulation.

**2.1. Prescribed performance constraint function.** Consider the following forms of a typical nonlinear control system:

$$\begin{aligned}\dot{x}_1 &= x_2 \\ \dot{x}_2 &= f + bu + d\end{aligned}\quad (1)$$

where  $x_1, x_2$  denote the system state,  $u$  is the control input,  $f$  is a function containing system states,  $b$  is a parameter containing system states and  $d$  is the external disturbance. In the nonlinear tracking control system, a typical control objective is to design the control input  $u$  so as to ensure that system state  $x_1$  converges to  $x_{1d}$  and  $x_2$  converges to zero. In the control process of the nonlinear system, the state of the nonlinear system, such as the convergence rate and the steady state error, should ideally satisfy some requirements in the control process, similar to the analysis of linear systems. A prescribed performance constraint function  $\lambda(t)$  is designed to ensure the system tracking error  $e = x_1 - x_{1d}$  converges to the prescribed performance. Therefore, the control objective of system (1) can be written as

$$\begin{aligned}1. & x_1 \rightarrow x_{1d} \\ 2. & x_2 \rightarrow 0 \\ 3. & -\lambda(t) < e = x_1 - x_{1d} < \lambda(t)\end{aligned}\quad (2)$$

Similar to [29], the prescribed performance constraint function can be designed as

$$\lambda(t) = (\lambda(0) - \lambda(\infty))e^{-lt} + \lambda(\infty)\quad (3)$$

where  $l$  is a positive constant and  $\lambda(0)$  is the initial value of the prescribed performance constraint function. Let  $e(0)$  denote the initial value of the state tracking error in system (1).  $\lambda(0)$  satisfies  $0 < |e(0)| < \lambda(0)$ ,  $\lambda(\infty) < \lambda(0)$ ,  $\lambda(\infty) > 0$ .

The prescribed performance constraint function is shown in Figure 1.

Figure 2 shows the prescribed performance constraint function under different values of  $l$  and  $\lambda(\infty)$ .

As shown in Figure 2, the value of  $l$  determines the convergence rate of the prescribed performance function: the larger the value of  $l$ , the faster the convergence rate.  $\lambda(\infty)$  determines the bound of the prescribed performance constraint function in the steady state.

Similar to the design of collision-avoidance functions in research on spacecraft collision-avoidance control, an error variable function is designed as follows:

$$\begin{aligned}\chi(t) &= \frac{e(t)}{\lambda(t)} \\ h(t) &= \left( \frac{1}{1 - \chi(t)^2} \right)^2, \quad t = \{t \mid |e(t)| < \lambda(t)\}\end{aligned}\quad (4)$$

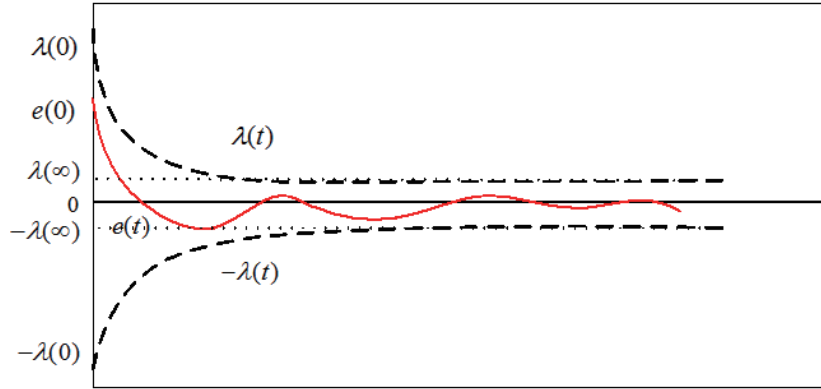


FIGURE 1. Prescribed performance constraint function

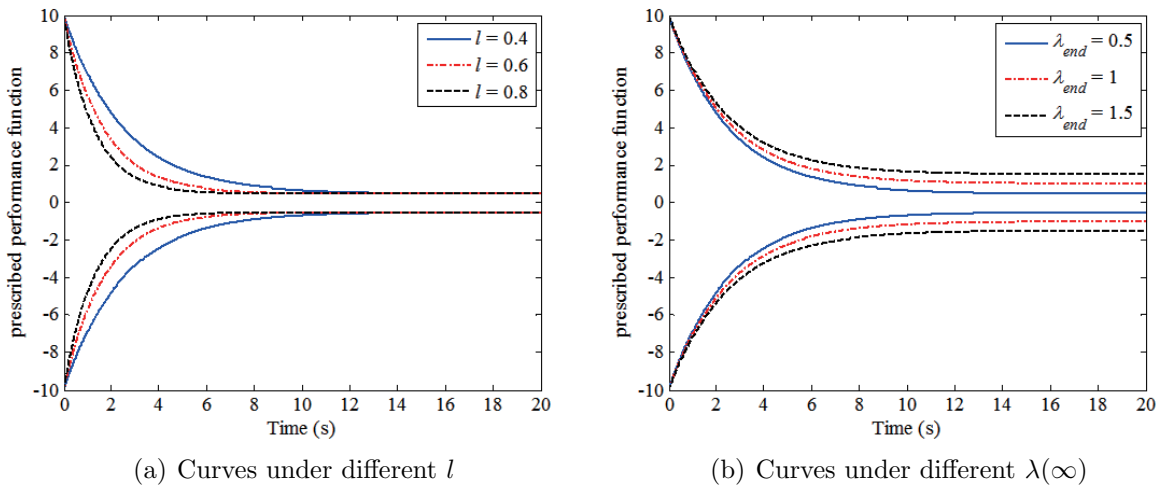


FIGURE 2. Prescribed performance constraint function under different parameter values

As  $e(0) < \lambda(0)$ ,  $\chi^2(0) < 1$ . Thus,  $h(0)$  exists in the definition domain

$$t = \{0 < t < t = t \mid \max\{|e(t)| < \lambda(t)\}\},$$

and the derivative of  $h(t)$  in the definition domain can be written as

$$\dot{h}(t) = \frac{4\lambda^3 e (\lambda \dot{e} - \dot{\lambda} e)}{(\lambda^2 - e^2)^3} \tag{5}$$

**Remark 2.1.** To ensure the system tracking error satisfies  $\left| \frac{e(t)}{\lambda(t)} \right| < 1$ , as  $h(0)$  exists, it is only necessary to ensure that  $h(t)$  is bounded in the process of system convergence.

Therefore, the state constraint problem for the tracking control of nonlinear systems is transformed into the design of controller to ensure that  $h(t)$  is bounded in the process of system convergence.

**2.2. Guidance system models with target maneuvering.** Figure 3 shows the two-dimensional homing guidance geometry. In this figure,  $O$  is the missile and  $T$  is the target.  $R$  represents the relative distance between the target and the missile. The speed and lateral acceleration of the missile and the target are denoted as  $(V_m, a_m)$  and  $(V_t, a_t)$ , respectively.  $\theta_m$  and  $\theta_t$  denote the direction of  $V_m$  and  $V_t$  with respect to the LOS frame.

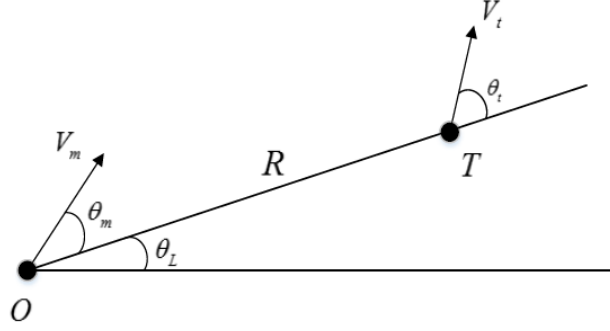


FIGURE 3. Geometry in two-dimensional space

It is assumed that the origin is the missile launch point. The engagement dynamics are given as follows:

$$\dot{R} = V_t \cos(\theta_t) - V_m \cos(\theta_m) \quad (6)$$

$$R\dot{\theta}_L = V_t \sin(\theta_t) - V_m \sin(\theta_m) \quad (7)$$

$$\dot{\theta}_m = \frac{a_m}{V_m} - \dot{\theta}_L \quad (8)$$

$$\dot{\theta}_t = \frac{a_t}{V_t} - \dot{\theta}_L \quad (9)$$

The main purpose of this paper is to design sliding mode guidance laws with prescribed performance. In other words, the lateral acceleration of the missile is designed to ensure that the missile intercepts the target at a designated angle  $\theta_{Lf}$ , and that the LOS angle tracking error  $\theta_L - \theta_{Lf}$  converges according to the prescribed performance.

In this paper, the signals  $R$ ,  $\dot{R}$ ,  $\theta_L$ ,  $\dot{\theta}_L$  and  $\theta_m$  are assumed to be measurable. Let  $\theta_{Lf}$  be the desired LOS angle,  $x_1 = \theta_L - \theta_{Lf}$  be the LOS angle error, and  $x_2 = \dot{\theta}_L$  be the LOS angular rate.

By differentiating (7) and rearranging dynamic Equations (6)-(9), the guidance system considering the prescribed performance constraint problem can be rewritten as

$$\begin{cases} \dot{x}_1 = x_2 \\ \dot{x}_2 = f + ba_m + d \end{cases} \quad (10)$$

where  $f = -\frac{2\dot{R}}{R}x_2$ ,  $b = -\frac{\cos(\theta_m)}{R}$ ,  $d = \frac{\cos(\theta_t)}{R}a_t$ .

This formula establishes the relationship between the line-of-sight angular rate  $\dot{\theta}_L$  and the normal acceleration  $a_m$  of the missile.  $f$  is a quantity containing the system states,  $b$  is a time-varying parameter,  $d$  is a parameter containing maneuvering information  $a_t$  of the target, and  $d$  is regarded as the disturbance of the system to design the controller.

**2.3. Related assumptions and lemmas.** To facilitate the design, the following lemmas and assumptions are stated.

**Lemma 2.1.** [34]. *Consider the nonlinear system  $\dot{x} = f(x, t)$ ,  $x \in R^n$ . Suppose that there exists a continuous and positive definite function  $V(x)$  such that*

$$\dot{V}(x) \leq -\mu V(x) - \lambda V^\alpha(x) \quad (11)$$

where  $\mu, \lambda > 0$  and  $0 < \alpha < 1$  are constants.  $x(t_0) = x_0$ , where  $t_0$  is the initial time. The system states arrive at the equilibrium point at time  $T$ , which satisfies the following inequality:

$$T \leq \frac{1}{\mu(1-\alpha)} \ln \frac{\mu V^{1-\alpha}(x_0) + \lambda}{\lambda} \quad (12)$$

That is, the system states are finite-time convergent.

**Lemma 2.2.** [35]. Consider the system  $\dot{x} = f(x, t)$ ,  $x \in \mathbb{R}^n$ . Suppose that there exists a Lyapunov function  $V(x)$  and scalars  $\varepsilon \in (0, 1)$ ,  $c > 0$ , and  $0 < \delta < \infty$  such that

$$\dot{V} \leq -cV^\varepsilon + \delta \quad (13)$$

Then, the trajectory of this system is practical finite-time stable.

**Assumption 2.1.** The target acceleration  $a_t$  is assumed to be bounded and to satisfy  $|a_t| < d_{\max}$ , where  $d_{\max}$  is the upper bound of the target acceleration.

**Assumption 2.2.** During the time horizon of the guidance process,  $\dot{R} < 0$ ,  $0 < R < R(0)$ , and  $t > 0$ . The missile intercepts the target when  $R \neq 0$ , but belongs to the interval  $[r_{\min}, r_{\max}] = [0.1m, 0.25m]$  [36].

**3. Guidance Law Design.** Different from the funnel control theory and the PPC theory, this section transforms the prescribed performance constraint problem into the boundedness of the error variable function and a new sliding mode surface is designed to ensure the boundedness of the variable function. First, some definitions and basic properties are stated. Let  $\tanh(\cdot)$  denote the hyperbolic tangent function and  $\cosh(\cdot)$  denote the hyperbolic cosine function. Referring to [37], a simple derivation procedure  $\forall \mathbf{x} \in \mathbb{R}^n$ ,  $y \in \mathbb{R}$  leads to the following basic properties:

$$x \cdot \tanh(x) \geq \tanh(x)^2 \geq 0 \text{ (equality occurs when } x = 0) \quad (14)$$

$$\frac{d \tanh(y)}{dy} = \left( \frac{1}{\cosh(y)} \right)^2 = \cosh^{-2}(y), \cosh(y) \geq 1, -1 \leq \tanh(y) \leq 1 \quad (15)$$

where  $\tanh(x) = \frac{\sinh(x)}{\cosh(x)} = \frac{e^x - e^{-x}}{e^x + e^{-x}}$ ,  $\cosh(x) = \frac{e^x + e^{-x}}{2}$ .

**3.1. Design of sliding mode guidance law with prescribed performance.** The main objective of this study is to design guidance laws so that the missile can intercept a maneuvering target at a desired LOS angle  $\theta_{Lf}$  with prescribed performance  $\left| \frac{e(t)}{\lambda(t)} \right| < 1$ . Let  $e = x_1 = \theta_L - \theta_{Lf}$ ,  $\dot{e} = \dot{\theta}_L$ . The sliding mode surface is designed as follows:

$$S = k_1 \tanh(\rho \dot{e}) + (k_2 h + k_3) e \quad (16)$$

where  $k_1$ ,  $k_2$ ,  $k_3$  and  $\rho$  are positive constants to be determined.

The derivative of  $S$  can be expressed as

$$\dot{S} = k_1 \rho \cosh^{-2}(\rho \dot{e}) \ddot{e} + k_2 \dot{h} e + (k_2 h + k_3) \dot{e} \quad (17)$$

The design idea presented in this paper is to use the boundedness of  $S$  to ensure the error variable function  $h(t)$  is bounded. If the upper bound  $d_{\max}$  of the target maneuvers is known, the finite-time guidance law of a missile intercepting maneuvering targets at a desired LOS angle with prescribed performance can be expressed, under Assumptions 2.1 and 2.2, using the following equation:

$$u_1 = b^{-1} \left[ -f - (\rho k_1)^{-1} \cosh^2(\rho \dot{e}) \left( k_2 \dot{h} e + (k_2 h + k_3) \dot{e} + k_4 S + k_5 \text{sign}(S) \right) \right] \quad (18)$$

where  $k_4$  and  $k_5$  are positive constants, and  $k_5$  is chosen such that  $k_5 > \rho k_1 d_{\max}$ .

**Theorem 3.1.** Considering the system in (6)-(9), if Assumptions 2.1 and 2.2 hold, and the external disturbance  $a_t$  is bounded, then  $|a_t| < d_{\max}$ . If (16) is selected as the sliding mode surface and (18) is selected as the guidance law, the following conclusions can be drawn:

(i) The sliding mode surface  $S$  converges to zero in finite time;

(ii) The LOS tracking error  $\theta_L - \theta_{Lf}$  and the LOS angular rate asymptotically converge to zero;

(iii) In the whole guidance process, the LOS tracking error  $e = \theta_L - \theta_{Lf}$  always satisfies  $\left| \frac{e(t)}{\lambda(t)} \right| < 1$ .

**Proof:** Using Assumption 2.1 and the property of the  $\cosh(\cdot)$  function,

$$S \cosh^{-2}(\rho\dot{e})d \leq |S| d_{\max} \quad (19)$$

Consider the Lyapunov function candidate as

$$V_1 = \frac{1}{2}S^2 \quad (20)$$

The time derivative of  $V_1$  along with (6)-(9) gives

$$\dot{V}_1 = S\dot{S} = S \left[ k_1\rho \cosh^{-2}(\rho\dot{e})\ddot{e} + k_2\dot{h}e + (k_2h + k_3)\dot{e} \right] \quad (21)$$

Using inequality (19) and substituting the controller of (18) into (21), we obtain

$$\begin{aligned} \dot{V}_1 &= S \left[ k_1\rho \cosh^{-2}(\rho\dot{e})\ddot{e} + k_2\dot{h}e + (k_2h + k_3)\dot{e} \right] \\ &= S \left[ k_1\rho \cosh^{-2}(\rho\dot{e})d - k_4S - k_5\text{sign}(S) \right] \\ &\leq -k_4S^2 - k_5S \cdot \text{sign}(S) + k_1\rho |S| d_{\max} \\ &\leq -k_4S^2 - (k_5 - k_1\rho d_{\max}) |S| \\ &\leq -aV_1 - bV_1^{\frac{1}{2}} \end{aligned} \quad (22)$$

where  $a = 2k_4 > 0$ ,  $b = \sqrt{2}(k_5 - k_1\rho d_{\max}) > 0$ . According to Lemma 2.1, inequality (22) indicates that the sliding manifold  $S$  converges to zero in finite time. Thus, conclusion (i) has been proved.

The stability analysis of the tracking error  $e$  is as follows.

Case 1. If  $\dot{e} = 0$ , using  $S = 0$  and (16) implies that  $e = 0$ . This means that the LOS angle tracking error  $e$  converges to zero.

Case 2. If  $\dot{e} \neq 0$ , consider the Lyapunov function  $V_2$  candidate as

$$V_2 = \frac{1}{2}e^2 \quad (23)$$

The derivative of  $V_2$  can be written as

$$\dot{V}_2 = e\dot{e} = -k_1(k_2h + k_3)^{-1}\dot{e} \tanh(\rho\dot{e}) \quad (24)$$

According to  $h(t) \geq 0$  and (14),

$$\dot{V}_2 = e\dot{e} = -k_1(k_2h + k_3)^{-1}\dot{e} \tanh(\rho\dot{e}) < 0 \quad (25)$$

From (25), the LOS angle tracking error  $e$  converges to zero asymptotically. Thus, the LOS angular rate converges to zero asymptotically. This proves conclusion (ii).

From the previous analyses, the sliding manifold  $S$  converges to zero in finite time. Therefore,  $S$  is bounded in the tracking control process. The boundedness of the  $\tanh(\cdot)$  function means that  $k_1 \tanh(\rho\dot{e})$  is bounded. Therefore,  $(k_2h + k_3)e$  is bounded. Next, the boundedness of the error variable function  $h(t)$  is proved using reduction to absurdity.

Assuming that there exists a certain time point  $t_p$  that makes  $h(t)$  unbounded in the convergence process of the system, (4) implies that  $\left| \frac{e(t_p)}{\lambda(t_p)} \right| = 1$ ,  $|e(t_p)| = |\lambda(t_p)|$ . Therefore, at time  $t_p$ ,  $(k_2h + k_3)e$  is unbounded, which contradicts the previous conclusions. Additionally, when  $e(t) = 0$ ,  $h(t) = 1$ . Hence,  $h(t)$  is always bounded in the tracking

control process. Thus, conclusion (iii) has been proved. This completes the proof of all conclusions in Theorem 3.1.

**Remark 3.1.** *In the above design process, the boundedness of the sliding mode surface  $S$  is used to deduce that  $h(t)$  is always bounded in the process of system convergence, which means that as long as  $|e(0)| < \lambda(0)$ ,  $\left|\frac{e(t)}{\lambda(t)}\right| < 1$  is always satisfied in the process of system convergence. However, during the design process, if  $e(t)$  is too close to  $\lambda(t)$ , then  $h(t)$  may become too large, which requires the controller to ensure better performance. Therefore, the parameter  $k_2$  in front of  $h(t)$  in controller  $u$  should not be too large.*

**Remark 3.2.** *In Theorem 3.1, it is assumed that the upper bound of the external disturbance in the guidance system is known. However, in practice, the upper bound of  $d$  (including  $a_t$  and  $\theta_t$ ) cannot be accurately measured or estimated. To solve this problem, adaptive control is introduced to design the guidance law.*

**3.2. Design of adaptive sliding mode guidance law with prescribed performance.** To solve the problem of the upper bound of the external disturbance being unknown, an adaptive control method is used to estimate the upper bound of the target accelerations. The adaptive sliding mode guidance law is designed as (26), and the external disturbance  $d$  satisfies  $|d| \leq \bar{d}_M$ , where  $\bar{d}_M$  is an unknown positive constant and  $\hat{d}_M$  is the estimate of  $d_M$ . Let  $\tilde{d}_M = d_M - \hat{d}_M$ ,  $\delta = \rho k_1$  be the adaptive gain coefficient. Then,

$$u_2 = b^{-1} \left[ -f - (\rho k_1)^{-1} \cosh^2(\rho \dot{e}) \left( k_2 \dot{h}e + (k_2 h + k_3) \dot{e} + k_4 S + k_5 \text{sign}(S) + \rho k_1 \hat{d}_M \text{sign}(S) \right) \right] \tag{26}$$

$$\dot{\hat{d}}_M = \delta |S|, \quad \delta = \rho k_1 \tag{27}$$

**Theorem 3.2.** *Considering the system in (6)-(9), if Assumptions 2.1 and 2.2 hold, and the external disturbance  $a_t$  is bounded, then if (16) is selected as the sliding mode surface and (26) is selected as the guidance law, the following conclusions can be drawn:*

(i) *The sliding manifold  $S$  and the adaptive parameter  $\hat{d}_M$  are bounded, and  $\hat{d}_M$  has an upper bound of  $\bar{d}_M$ , which makes  $\hat{d}_M \leq \bar{d}_M$ ;*

(ii) *The sliding manifold  $S$  converges to zero in finite time, and the LOS tracking error  $\theta_L - \theta_{Lf}$  and the LOS angular rate asymptotically converge to within a small region of zero;*

(iii) *In the whole guidance process, the LOS tracking error  $e = \theta_L - \theta_{Lf}$  always satisfies  $\left|\frac{e(t)}{\lambda(t)}\right| < 1$ .*

**Proof:** Consider the Lyapunov function candidate to be

$$V_3 = \frac{1}{2} S^2 + \frac{1}{2} \tilde{d}_M^2 \tag{28}$$

Taking the time derivative of  $V_3$  along with (6)-(9) and substituting the controller of (26) and (16) into (28), we obtain

$$\begin{aligned} \dot{V}_3 &= S \dot{S} + \tilde{d}_M \dot{\tilde{d}}_M \\ &= S \left[ -k_4 S - k_5 \text{sign}(S) - \rho k_1 \hat{d}_M \text{sign}(S) + \rho k_1 \cosh^{-2}(\rho \dot{e}) d \right] + \tilde{d}_M \dot{\tilde{d}}_M \\ &\leq -k_4 S^2 - k_5 |S| - \rho k_1 \hat{d}_M |S| + \rho k_1 d_M |S| + \tilde{d}_M \dot{\tilde{d}}_M \\ &\leq -k_4 S^2 - k_5 |S| + \rho k_1 \tilde{d}_M |S| - \dot{\tilde{d}}_M \tilde{d}_M \end{aligned} \tag{29}$$



$$\begin{aligned} &\leq -k_4 S^2 - k_5 |S| + \rho k_1 \hat{d}_M |S| - \rho k_1 \bar{d}_M |S| \\ &\leq -k_4 S^2 - k_5 |S| \\ &\leq 0 \end{aligned}$$

According to inequality (29), the sliding manifold  $S$  and  $\hat{d}_M$  are bounded, and so the adaptive parameter  $\hat{d}_M$  has an upper bound. This means that there exists a positive constant  $\bar{d}_M > 0$  that satisfies  $\hat{d}_M \leq \bar{d}_M$ . Thus, conclusion (i) has been proved.

Consider the Lyapunov function candidate  $V_4$  to be

$$V_4 = \frac{1}{2} S^2 + \frac{1}{2} (\bar{d}_M - \hat{d}_M)^2 \tag{30}$$

The derivative of  $V_4$  is

$$\begin{aligned} \dot{V}_4 &= S\dot{S} - \dot{\hat{d}}_M (\bar{d}_M - \hat{d}_M) \\ &= S \left[ -k_4 S - k_5 \text{sign}(S) - \rho k_1 \hat{d}_M \text{sign}(S) + \rho k_1 \cosh^{-2}(\rho \dot{e}) d \right] - \dot{\hat{d}}_M (\bar{d}_M - \hat{d}_M) \\ &\leq -k_4 S^2 - k_5 |S| - \rho k_1 \hat{d}_M |S| + \rho k_1 d_M |S| - \dot{\hat{d}}_M (\bar{d}_M - \hat{d}_M) \\ &\leq -k_4 S^2 - k_5 |S| + \rho k_1 (\bar{d}_M - \hat{d}_M) |S| - \dot{\hat{d}}_M (\bar{d}_M - \hat{d}_M) \\ &\leq -k_5 |S| - (\bar{d}_M - \hat{d}_M) + (\bar{d}_M - \hat{d}_M) \\ &\leq -\min(\sqrt{2}k_5, \sqrt{2}) V_4^{\frac{1}{2}} + \delta \end{aligned} \tag{31}$$

where  $\delta = (\bar{d}_M - \hat{d}_M)$ .

As  $\bar{d}_M$  and  $\hat{d}_M$  are bounded,  $\delta$  is bounded. According to Lemma 2.2,  $V_4$  is practical finite-time stable. This means that the sliding manifold  $S$  is practical finite-time stable. Hence, the sliding manifold  $S$  converges to a region  $|S| \leq \Delta$ , where  $\Delta$  is an unknown positive constant. The stability analyses of  $e$  and  $\dot{e}$  are as follows.

According to (16),

$$S = k_1 \tanh(\rho \dot{e}) + (k_2 h + k_3) e = \Delta_1 \tag{32}$$

where  $|\Delta_1| \leq \Delta$ . Equation (32) can be written as

$$k_1 \tanh(\rho \dot{e}) = -(k_2 h + k_3) e + \Delta_1 = -(k_2 h + k_3) \left( e - \frac{\Delta_1}{(k_2 h + k_3)} \right) \tag{33}$$

As the parameters  $k_1, k_2, k_3, \rho$ , and  $h(t)$  are greater than zero,  $k_1 \tanh(\rho \dot{e})$  and  $\dot{e}$  have the same sign. Thus, if  $e - \frac{\Delta_1}{(k_2 h + k_3)} > 0$ , that is,  $e > \frac{\Delta_1}{(k_2 h + k_3)}$ , then  $\dot{e} < 0$ . If  $e - \frac{\Delta_1}{(k_2 h + k_3)} < 0$ , then  $\dot{e} > 0$ . Therefore, the system state  $e$  will converge to a region  $\frac{\Delta_1}{(k_2 h + k_3)}$ . Because of the boundedness and monotonicity of the  $\tanh(\cdot)$  function,  $\dot{e}$  will converge to a small region around zero. Thus, conclusion (ii) has been proved.

From the previous analyses, the sliding manifold  $S$  is bounded in the tracking control process. From the boundedness of the  $\tanh(\cdot)$  function,  $k_1 \tanh(\rho \dot{e})$  is bounded. Therefore,  $(k_2 h + k_3) e$  is bounded. Similar to the proof of Theorem 3.1, it can be shown that  $h(t)$  is always bounded in the tracking control process. Thus, conclusion (iii) has been proved. This completes the proof of all conclusions in Theorem 3.2.

**Remark 3.3.** *Because of the presence of the sign function in this formulation, the chattering problem may occur. To weaken this phenomenon, a continuous function such as*

(34) can be used in replace of the sign function.

$$\text{sat}(S) = \begin{cases} 1, & S > \sigma \\ S/\sigma, & |S| \leq \sigma \\ -1, & S < -\sigma \end{cases} \quad (34)$$

where  $\sigma$  is a small positive constant.

**4. Simulations.** This section reports the results of simulations to verify the proposed guidance laws with prescribed performance. To illustrate the effectiveness of the designed guidance laws, two different target maneuvering scenarios are considered.

Case 1:  $a_t = 5g \cos(t)$  m/s<sup>2</sup>

Case 2:  $a_t = 5g$  m/s<sup>2</sup>

where  $g = 9.8$  m/s<sup>2</sup> denotes the acceleration of gravity.

To verify the performance of the designed guidance laws, the results are compared with those from the proportional navigation guidance law (PNGL) and fast nonsingular terminal sliding mode guidance law (FNTSMGL) [38].

The PNGL is given as

$$n_c = -N\dot{R}\dot{\theta}_L \quad (35)$$

The fast nonsingular terminal sliding mode surface is given as

$$S = \dot{x} + \alpha_1 x + \alpha_2 f(x) \quad (36)$$

$$f(x) = \begin{cases} r_1 x + r_2 x^2 \text{sign}(x) & |x| < \eta \\ |x|^r \text{sign}(x) & \text{otherwise} \end{cases} \quad (37)$$

$$r_1 = (2 - r)\eta^{r-1} \quad (38)$$

$$r_2 = (r - 1)\eta^{r-2} \quad (39)$$

where  $r$ ,  $\alpha_1$ ,  $\alpha_2$ , and  $\eta$  are positive constants,  $0 < r < 1$ .

The FNTSMGL is given as

$$u_0 = -b^{-1} \left( f + \alpha_1 \dot{x} + \alpha_2 \dot{\beta}(x) + k_1 S + k_2 \text{sign}(S) \right) \quad (40)$$

$$\dot{\beta}(x) = \begin{cases} r_1 \dot{x} + 2r_2 x \dot{x} \text{sign}(x) & |x| < \eta \\ r |x|^{r-1} \dot{x} & \text{otherwise} \end{cases} \quad (41)$$

In order to demonstrate that the guidance law designed in this paper is still valid under different scenarios, the two sets of initial scene parameters listed in Table 1 are considered. Usually the speed of the missile is greater than that of the target. The first set of parameters is the terminal guidance for intercepting the subsonic cruise missile, and the second set of parameters is the terminal guidance for intercepting the maneuvering fighter.

TABLE 1. Initial scene parameters

Dataset	$R(0)$ , m	$\theta_L(0)$ , °	$\theta_m(0)$ , °	$\theta_t(0)$ , °	$\theta_{Lf}$ , °	$V_m$ , m/s	$V_t$ , m/s
1	5000	30	20	-20	20	600	300
2	9000	20	25	10	15	800	450

In practice, the control force provided by the dynamic actuators is limited. Therefore, the maximum lateral accelerations of the missile are assumed to be limited as

$$a_M = \begin{cases} a_{M \max} \text{sign}(a_M) & \text{if } |a_M| \geq a_{M \max} \\ a_M & \text{if } |a_M| < a_{M \max} \end{cases} \quad (42)$$

where  $a_{M \max} = 25g$ . This means that the maximum lateral acceleration of the missile is  $25g$ .

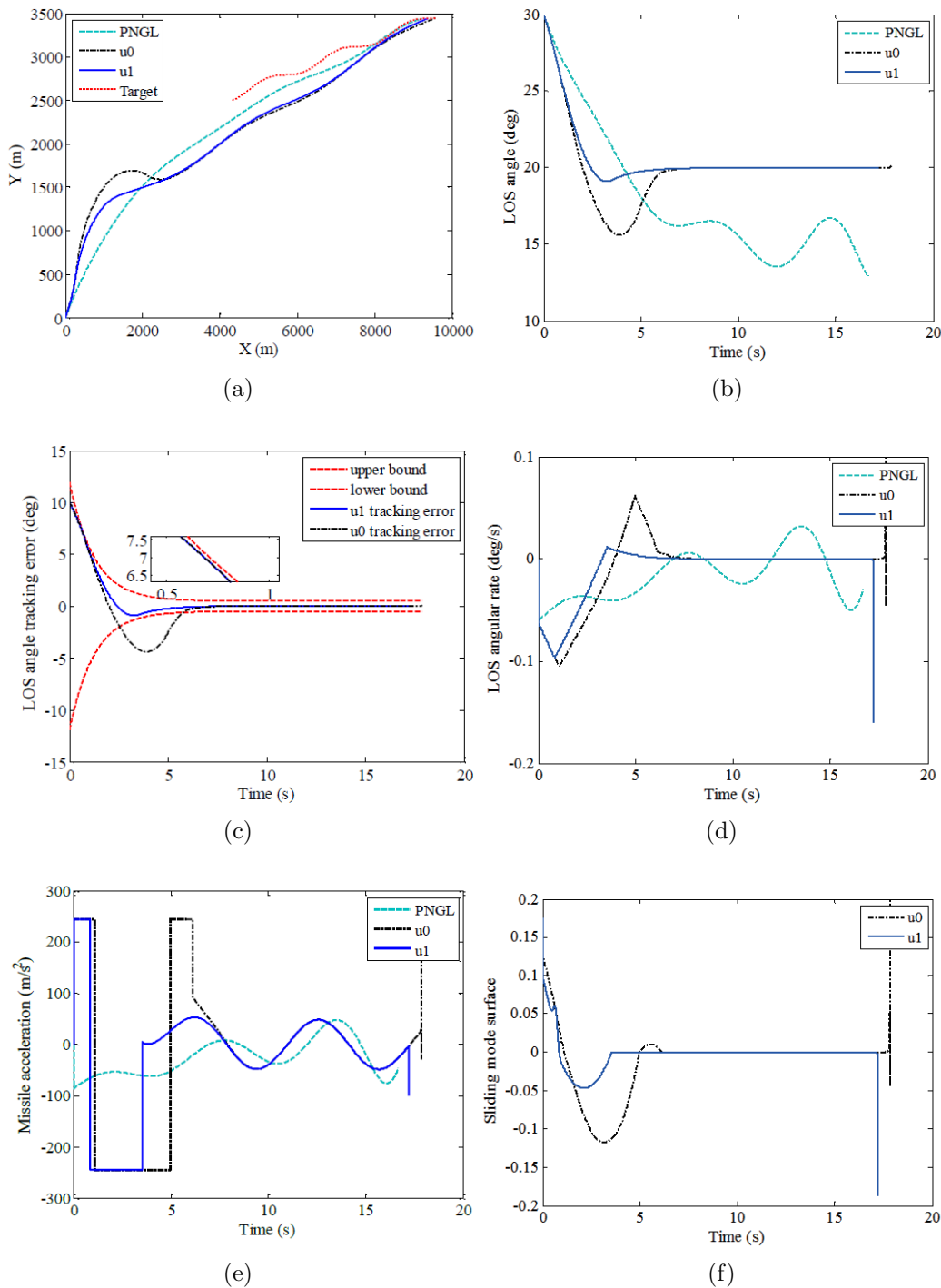
**4.1. Simulation results of sliding mode guidance law with prescribed performance.** The parameters of guidance law  $u_1$  are  $\rho = 2.45$ ,  $k_1 = 0.5$ ,  $k_2 = 0.0005$ ,  $k_3 = 1$ ,  $k_4 = 0.6$ ,  $k_5 = 2.7$ . The parameter in the saturation function is  $\sigma = 0.005$ . The parameters in the prescribed performance constraint function are  $\lambda(0) = 12$ ,  $\lambda(\infty) = 0.5$ ,  $l = 0.8$ . The initial scene parameters are given by dataset 1. The parameters in the FNTSMGL  $u_0$  are  $\alpha_1 = 0.02$ ,  $\alpha_2 = 0.39$ ,  $r = 0.4$ ,  $\eta = 0.25$ ,  $k_1 = 6$ ,  $k_2 = 2$ . The parameter in the PNGL is  $N = 5$ .

Case 1. When  $a_t = 5g \cos(t)$  m/s<sup>2</sup>, the target is performing an S-type maneuver. The simulation results under  $u_1$  are shown in Figure 4. Figure 4(a) shows the relative movement trajectories under three guidance laws. Although the flight trajectories of the missile are different, the three guidance laws can intercept the target successfully, which verifies the effectiveness of the guidance law presented in this paper. From Figure 4(b), the LOS angle converges to the desired angle under guidance laws  $u_1$  and  $u_0$ , but the PNGL cannot ensure the convergence of the LOS angle. Figure 4(c) shows the curves of the LOS tracking error for guidance laws  $u_1$  and  $u_0$  with the prescribed performance constraint function. The results indicate that the LOS angle tracking error converges to zero with the prescribed performance under guidance law  $u_1$ . However,  $u_0$  cannot guarantee the LOS tracking error converges to the prescribed performance. Figure 4(d) shows the curves of LOS angular rate  $\dot{\theta}_L$ . Good convergence performance is clearly observed under  $u_1$ . Figure 4(e) describes the acceleration of the missile. The acceleration under  $u_1$  and  $u_0$  exhibits saturation at the beginning of the guidance process. This is because the selected sliding mode surface requires a large control input to ensure rapid convergence. Figure 4(f) shows the sliding mode surface under  $u_1$  and  $u_0$ . Both surfaces converge to a small region in a short period of time. This is consistent with the previous theoretical analysis.

Case 2. For  $a_t = 5g$  m/s<sup>2</sup>, the simulation results under  $u_1$  are shown in Figure 5. Figure 5(a) indicates that the target is maneuvering in a different way, and that the missile can still intercept the target successfully under all three guidance laws. Figure 5(b) shows the curves of  $\theta_L$ . The LOS angle converges to the desired angle under  $u_1$  and  $u_0$ . The LOS angle tracking error with the prescribed performance is presented in Figure 5(c). Similar to case 1,  $u_1$  can still ensure the LOS angle tracking error converges to the prescribed performance. Figure 5(d) describes the LOS angular rate  $\dot{\theta}_L$ , and Figure 5(e) shows the acceleration of the missile under the three guidance laws. The final variation trend of the control input is related to the maneuvering of the target. As shown in Figure 5(f), the sliding mode surface under  $u_1$  and  $u_0$  converges to a small region within a short period of time.

In conclusion, it has been verified that the guidance law  $u_1$  designed in this paper performs well when the target is maneuvering in different ways. Compared with previously designed sliding mode guidance laws,  $u_1$  can ensure the LOS angle tracking error converges according to the prescribed performance. However, guidance law  $u_1$  requires the upper bound of the maneuvering information of the target to be known in advance. Considering that the parameters related to the target cannot be easily obtained in actual guidance systems, the next section describes simulations using the adaptive sliding mode guidance law with prescribed performance.

**Remark 4.1.** *As seen from the conclusions of Theorem 3.1 and Theorem 3.2, all the control parameters can have important effects on the control performance. However, due to the complexity of nonlinear system, there are still no explicit rules to amend the control parameters for the guidance control system. Therefore various trials have been made so*

FIGURE 4. Responses under  $u_1$  for Case 1

that the simulation results are acceptable. But to make the comparison results convincing and fair, the parameters must share the same values even under different simulation groups.

**4.2. Simulation results of adaptive sliding mode guidance law with prescribed performance.** Similar to Section 4.1, the PNGL and FNTSMGL  $u_0$  are compared with guidance law  $u_2$ . To separate this experiment from the simulation of  $u_1$ , dataset 2 in Table 1 is used as the initial scene parameters for the simulation. The parameters in

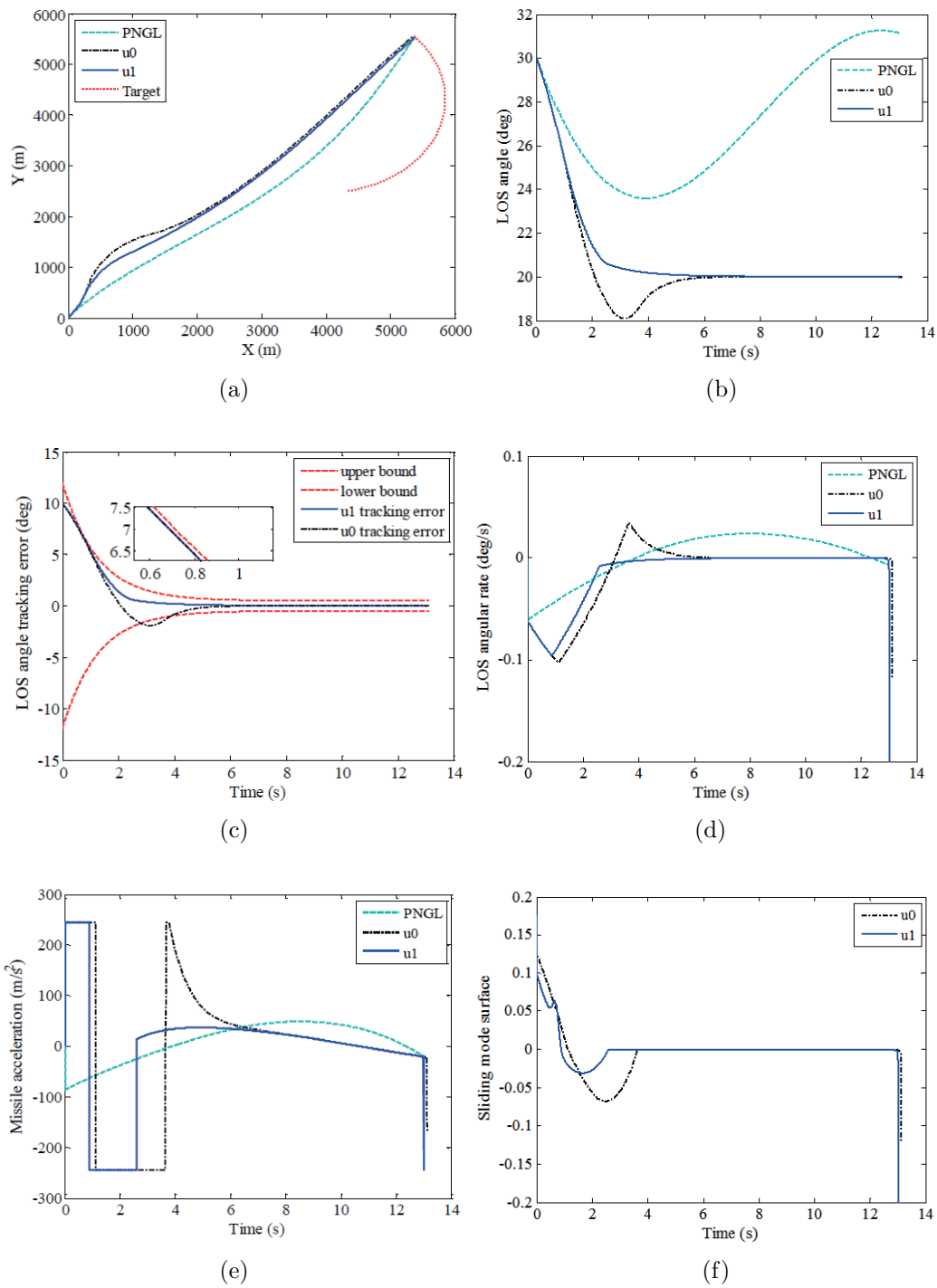


FIGURE 5. Responses under  $u_1$  for Case 2

guidance law  $u_2$  are the same as those for  $u_1$ :  $\rho = 2.45$ ,  $k_1 = 0.5$ ,  $k_2 = 0.0005$ ,  $k_3 = 1$ ,  $k_4 = 0.6$ ,  $k_5 = 2.7$ . The adaptive gain  $\delta = \rho k_1$ . The parameter in the saturation function is  $\sigma = 0.005$ . The parameters in the prescribed performance constraint function are  $\lambda(0) = 7$ ,  $\lambda(\infty) = 0.5$ ,  $l = 0.8$ . The parameters in guidance law  $u_0$  are  $\alpha_1 = 0.02$ ,  $\alpha_2 = 0.39$ ,  $r = 0.4$ ,  $\eta = 0.25$ ,  $k_1 = 6$ ,  $k_2 = 2$ . The parameter in the PNGL is  $N = 5$ .

Case 1. When  $a_t = 5g \cos(t)$  m/s<sup>2</sup>, the target is performing an S-type maneuver. The simulation results under  $u_2$  are shown in Figure 6. Figure 6(a) shows the relative movement trajectories under  $u_0$ , PNGL, and  $u_2$ . The missile can intercept the target

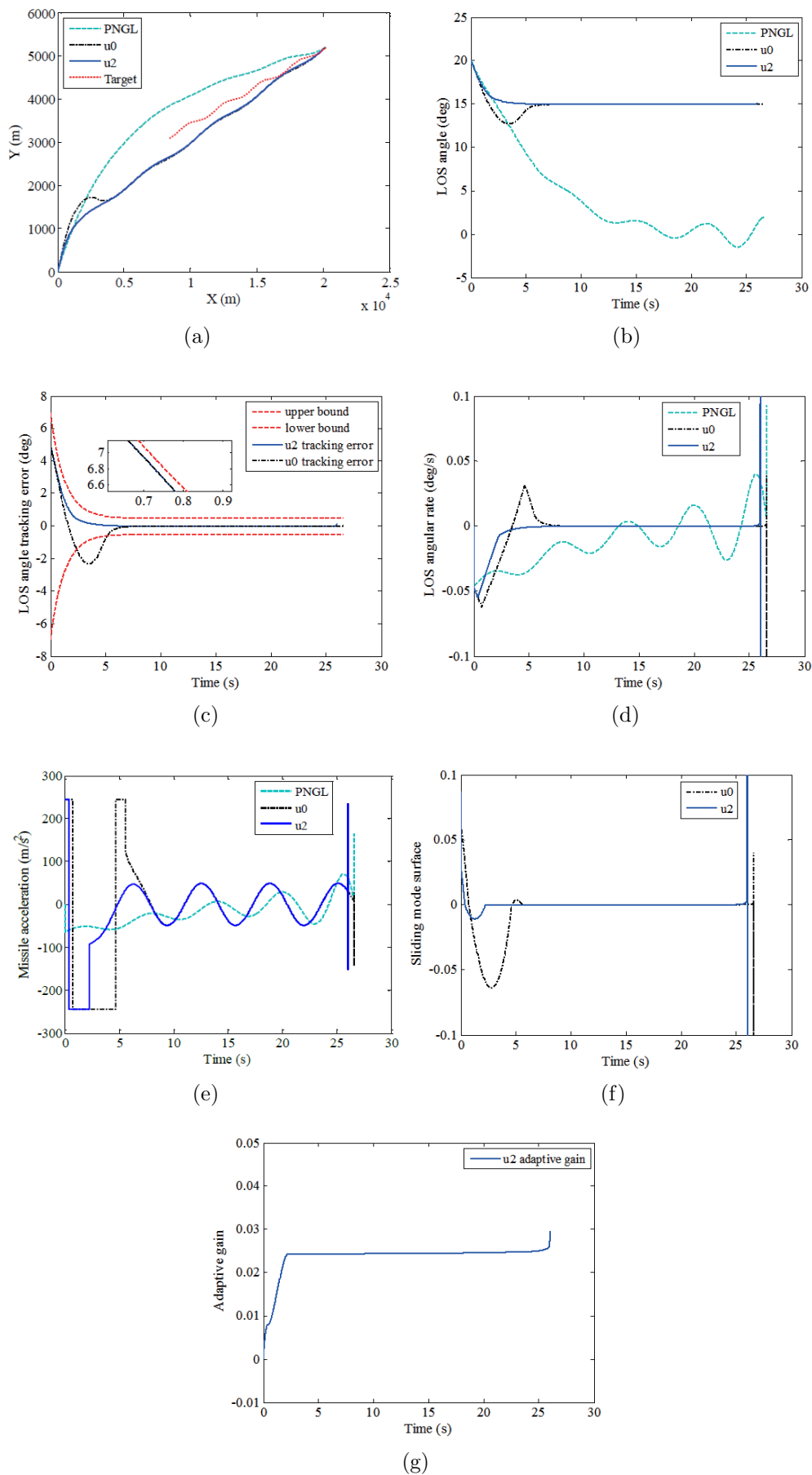


FIGURE 6. Responses under  $u_2$  for Case 1

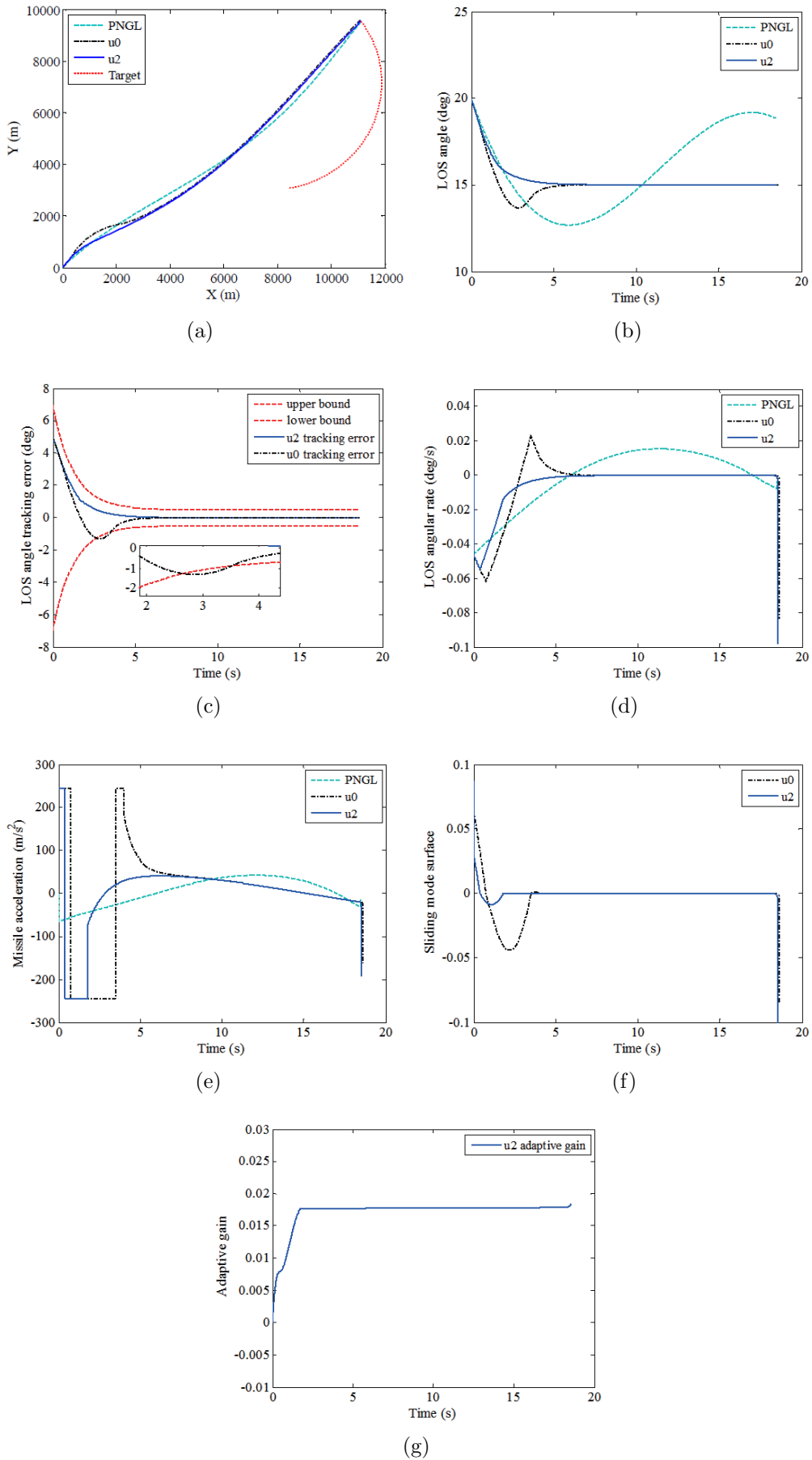


FIGURE 7. Responses under  $u_2$  for Case 2

successfully under  $u_2$ . Figure 6(b) shows the curves of the LOS angle. Guidance laws  $u_2$  and  $u_0$  can ensure that the LOS angle converges to the desired angle. Figure 6(c) describes the LOS tracking error with the prescribed performance function. The results indicate that guidance law  $u_2$  can ensure the LOS tracking error converges to the prescribed performance, but  $u_0$  does not have this property. Figure 6(d) shows the curves of LOS angular rate  $\dot{\theta}_L$ . From Figure 6(e), the missile acceleration under  $u_2$  and  $u_0$  exhibits saturation at the beginning of the process, as the selected sliding manifold requires a large control force to ensure rapid convergence. The curves of the sliding mode surface under  $u_2$  and  $u_0$  are presented in Figure 6(f). Both the sliding mode surfaces converge to a small region in a short period of time. The adaptive gain is presented in Figure 6(g). It can be seen that, as the sliding mode surface tends to a small region, the adaptive gain tends to a constant value.

Case 2. For  $a_t = 5g \text{ m/s}^2$ , the simulation results under  $u_2$  are shown in Figure 7. Figure 7(a) shows that the missile can still intercept the target successfully under all three guidance laws. Figure 7(b) indicates that the LOS angle  $\theta_L$  converges to the desired angle  $\theta_{Lf}$  under  $u_2$  and  $u_0$ . Figure 7(c) shows that  $u_2$  can still ensure the LOS angle tracking error converges to zero to satisfy the prescribed performance. Figure 7(d) describes the LOS angular rate  $\dot{\theta}_L$ . Figure 7(e) presents the acceleration of the missile. As shown in Figure 7(f), the sliding mode surface under  $u_2$  and  $u_0$  converges to a small region in a short period of time. The adaptive gain under  $u_2$  is given in Figure 7(g). The adaptive gain tends to a constant value as the sliding mode surface tends to a small region.

From the simulation results of Figures 6 and 7, it can be concluded that guidance law  $u_2$  designed in this paper ensures that the LOS angle converges to the desired angle with the prescribed performance. This agrees with the analysis of the dynamic process of the guidance system. Note that the prescribed performance function can, in theory, be designed arbitrarily. However, in actual guidance systems, the parameters of the prescribed performance constraint function cannot be selected arbitrarily because of the limited overload capability of the missile. If the parameter  $l$  in the prescribed performance function is too large, the system will converge faster, requiring a larger control force. This may lead to the failure of the prescribed performance constraint function. Therefore, the parameters should be selected according to the requirements of the actual system.

**5. Conclusions.** This paper has introduced prescribed performance sliding mode guidance laws that use an error variable function and a novel sliding mode surface to ensure that a missile intercepts a maneuvering target. The guidance laws designed in this paper can deal with the problem of target acceleration under known and unknown bounds using adaptive control. Compared with previous prescribed performance control methods, the controller proposed in this paper has a simpler form and superior robustness and practicality. A strict theoretical proof was presented, and simulation results verified the effectiveness and superiority of the guidance laws designed in this paper. The proposed controller can also be conveniently used to deal with prescribed performance problems in other scenarios requiring nonlinear control, such as robot control systems. However, the overload of the missile is not limited in this paper and the prescribed performance control method proposed in this paper cannot effectively constrain the overshoot. In the next work, the guidance law with actuator saturation and overshoot constraint will be considered.

**Acknowledgment.** This work is supported by the China Aerospace Science and Technology Innovation Foundation (number JZ20160008) and the Major Program of Natural Science Foundation of China (number 61690210).



## REFERENCES

- [1] S. Rogers, Missile guidance comparison, *AIAA Guidance, Navigation, and Control Conference and Exhibit*, AIAA Paper, Rhode Island, AIAA 2004-4882, 2004.
- [2] A. Ratnoo and D. Ghose, State-dependent Riccati-equation-based guidance law for impact-angle-constrained trajectories, *Journal of Guidance, Control, and Dynamics*, vol.32, no.1, pp.320-326, 2009.
- [3] N. Harl and S. N. Balakrishnan, Impact time and angle guidance with sliding mode control, *IEEE Transactions on Control Systems Technology*, vol.20, no.6, pp.1436-1449, 2012.
- [4] M. Kim and K. V. Grider, Terminal guidance for impact attitude angle constrained flight trajectories, *IEEE Transactions on Aerospace and Electronic Systems*, vol.AES-9, no.6, pp.852-859, 1973.
- [5] B. S. Kim, J. G. Lee and H. S. Hah, Biased PNG law for impact with angular constraint, *IEEE Transactions on Aerospace and Electronic Systems*, vol.34, no.1, pp.277-288, 1998.
- [6] S. K. Jeong, S. J. Cho and E. G. Kim, Angle constraint biased PNG, *Proc. of Asian Control Conference*, pp.1849-1854, 2004.
- [7] K. S. Erer and O. Merttopçuoğlu, Indirect impact-angle-control against stationary targets using biased pure proportional navigation, *Journal of Guidance, Control, and Dynamics*, vol.35, no.2, pp.700-704, 2012.
- [8] C. K. Ryoo, H. Cho and M. J. Tahk, Closed-form solutions of optimal guidance with terminal impact angle constraint, *IEEE Conference on Control Applications*, Istanbul, Turkey, pp.504-509, 2003.
- [9] C. K. Ryoo, H. Cho and M. J. Tahk, Optimal guidance laws with terminal impact angle constraint, *Journal of Guidance, Control, and Dynamics*, vol.28, no.4, pp.724-732, 2005.
- [10] Y. I. Lee, C. K. Ryoo and E. Kim, Optimal guidance with constraints on impact angle and terminal acceleration, *AIAA Guidance, Navigation, and Control Conference and Exhibit*, AIAA Paper, Austin, TX, AIAA 2003-5795, 2003.
- [11] Y. I. Lee, S. H. Kim and M. J. Tahk, Optimality of linear time-varying guidance for impact angle control, *IEEE Transactions on Aerospace and Electronic Systems*, vol.48, no.4, pp.2802-2817, 2012.
- [12] E. J. Ohlmeyer, Control of terminal engagement geometry using generalized vector explicit guidance, *2003 American Control Conference*, Denver, CO, pp.396-401, 2003.
- [13] Y. Zhang, M. Sun and Z. Chen, Finite-time convergent guidance law with impact angle constraint based on sliding-mode control, *Nonlinear Dynamics*, vol.70, no.1, pp.619-625, 2012.
- [14] S. R. Kumar, S. Rao and D. Ghose, Nonsingular terminal sliding mode guidance with impact angle constraints, *Journal of Guidance, Control, and Dynamics*, vol.37, no.4, pp.1114-1130, 2014.
- [15] J. Song, S. Song and H. Zhou, Adaptive nonsingular fast terminal sliding mode guidance law with impact angle constraints, *International Journal of Control, Automation and Systems*, vol.14, no.1, pp.99-114, 2016.
- [16] Z. F. Gao, P. Yang and M. S. Qian, Iterative learning observer-based fault tolerant control approach for satellite attitude system with mixed actuator faults, *ICIC Express Letters*, vol.13, no.7, pp.635-643, 2019.
- [17] A. Ilchmann, E. P. Ryan and C. J. Sangwin, Tracking with prescribed transient behaviour, *ESAIM: Control, Optimisation and Calculus of Variations*, pp.471-493, 2002.
- [18] A. Ilchmann and E. P. Ryan, High-gain control without identification: A survey, *GAMM-Mitteilungen*, vol.31, no.1, pp.115-125, 2008.
- [19] C. P. Bechlioulis and G. A. Rovithakis, A low-complexity global approximation-free control scheme with prescribed performance for unknown pure feedback systems, *Automatica*, vol.50, no.4, pp.1217-1226, 2014.
- [20] N. Hopfe, A. Ilchmann and E. P. Ryan, Funnel control with saturation: Nonlinear SISO systems, *IEEE Transactions on Automatic Control*, vol.55, no.9, pp.2177-2182, 2010.
- [21] A. Ilchmann and E. P. Ryan, Performance funnels and tracking control, *International Journal of Control*, vol.82, no.10, pp.1828-1840, 2009.
- [22] A. Ilchmann, H. Logemann and E. P. Ryan, Tracking with prescribed transient performance for hysteretic systems, *Society for Industrial and Applied Mathematics*, vol.48, no.7, pp.4731-4752, 2010.
- [23] A. Ilchmann, E. P. Ryan and S. Trenn, Tracking control: Performance funnels and prescribed transient behaviour, *Systems and Control Letters*, vol.54, no.7, pp.655-670, 2005.
- [24] M. C. Hackl, N. Hopfe, A. Ilchmann, M. Mueller and S. Trenn, Funnel control for systems with relative degree two, *SIAM Journal on Control and Optimization*, vol.51, no.2, pp.965-995, 2010.
- [25] T. Reis and T. Berger, Funnel control via funnel pre-compensator for minimum phase systems with relative degree two, *IEEE Transactions on Automatic Control*, vol.63, no.7, pp.2264-2271, 2018.

- [26] C. P. Bechlioulis and G. A. Rovithakis, Robust adaptive control of feedback linearizable MIMO nonlinear systems with prescribed performance, *IEEE Transactions on Automatic Control*, vol.53, no.9, pp.2090-2099, 2008.
- [27] C. P. Bechlioulis and G. A. Rovithakis, Adaptive control with guaranteed transient and steady state tracking error bounds for strict feedback systems, *Automatica*, vol.45, no.2, pp.532-538, 2009.
- [28] C. P. Bechlioulis and G. A. Rovithakis, Prescribed performance adaptive control for multi-input multi-output affine in the control nonlinear systems, *IEEE Transactions on Automatic Control*, vol.55, no.5, pp.1220-1226, 2010.
- [29] C. P. Bechlioulis and G. A. Rovithakis, Reinforcing robustness of adaptive dynamic surface control, *International Journal of Adaptive Control and Signal Processing*, vol.27, no.4, pp.323-339, 2013.
- [30] Z. F. Gao, Z. P. Zhou, G. P. Jiang, M. S. Qian and J. X. Lin, Active fault tolerant control scheme for satellite attitude systems: Multiple actuator faults case, *International Journal of Control, Automation and Systems*, vol.16, no.4, pp.1794-1804, 2018.
- [31] L. J. Wang, W. Z. Jin and G. Y. Li, Three-dimensional adaptive dynamic surface guidance law against maneuvering targets with input constraints and second-order dynamics autopilot, *International Journal of Innovative Computing, Information and Control*, vol.14, no.5, pp.1725-1739, 2018.
- [32] H. B. Ji, X. D. Liu, Z. Y. Song and Y. Zhao, Time-varying sliding mode guidance scheme for maneuvering target interception with impact angle constraint, *Journal of the Franklin Institute*, vol.355, no.18, pp.9192-9208, 2018.
- [33] X. H. Li, S. S. Song and Y. Guo, Robust finite-time tracking control for Euler-Lagrange systems with obstacle avoidance, *Nonlinear Dynamics*, vol.93, no.2, pp.443-451, 2018.
- [34] S. Yu, X. Yu, B. Shirinzadeh and Z. H. Man, Continuous finite-time control for robotic manipulators with terminal sliding mode, *Automatica*, vol.44, no.11, pp.1957-1964, 2005.
- [35] Z. Zhu, Y. Xia and M. Fu, Attitude stabilization of rigid spacecraft with finite-time convergence, *International Journal of Robust and Nonlinear Control*, vol.21, no.6, pp.686-702, 2011.
- [36] Y. B. Shtessel, I. A. Shkolnikov and A. Levant, Guidance and control of missile interceptor using second-order sliding modes, *IEEE Transactions on Aerospace and Electronic Systems*, vol.45, no.1, pp.110-124, 2009.
- [37] N. Fischer, A. Dani, N. Sharma and W. E. Dixon, Saturated control of an uncertain nonlinear system with input delay, *Automatica*, vol.49, no.6, pp.1741-1747, 2013.
- [38] Y. Si and S. Song, Three-dimensional adaptive finite-time guidance law for intercepting maneuvering targets, *Chinese Journal of Aeronautics*, vol.30, no.6, pp.1985-2003, 2017.